AIMS Mathematics, 9(11): 31142–31162.
DOI: 10.3934/math.20241501
Received: 03 September 2024
Revised: 17 October 2024
Accepted: 23 October 2024
Published: 01 November 2024

https://www.aimspress.com/journal/Math

Research article

Exact solutions to the fractional nonlinear phenomena in fluid dynamics via the Riccati-Bernoulli sub-ODE method

Waleed Hamali[1] **and Abdulah A. Alghamdi**[2,3,*]

[1] Department of Mathematics, Faculty of Science, Jazan University, P.O. Box 2097, Jazan 45142, kingdom of Saudi Arabia

[2] Mathematical Modeling and Applied Computation (MMAC) Research Group, Department of Mathematics, King Abdulaziz University, Jeddah 21589, kingdom of Saudi Arabia

[3] Center of Modern Mathematical Sciences and their Applications (CMMSA), King Abdulaziz University, Jeddah 21589, kingdom of Saudi Arabia

* **Correspondence:** Email: aaalghamdi6@kau.edu.sa.

Abstract: The Riccati-Bernoulli sub-ODE method has been used in recent research to efficiently investigate the analytical solutions of a non-linear equation widely used in fluid dynamics research. By utilizing this method, exact solutions are obtained for the space-time fractional symmetric regularized long-wave equation. These results comprehensively understand the long wave equation widely used in numerous fluid dynamics and wave propagation scenarios. The approach to studying these phenomena and using conceptual representation to understand their essential characteristics opens the door to valuable insights that may help improve both the theoretical and applied aspects of fluid dynamics and similar fields. Thus, as these complex equations demonstrate, the suggested approach is a valuable tool for conducting further research into non-linear phenomena across several disciplines.

Keywords: nonlinear partial differential equations; Riccati-Bernoulli sub-ODE method; space-time fractional regularized long-wave equation; analytical solutions; wave propagation; exact solutions
Mathematics Subject Classification: 34G20, 35A20, 35A22, 35R11

1. Introduction

Accurately describing natural phenomena at small scales requires using fractional-order differential equations instead of their integer-order counterparts. The need to formulate fractional ordinary differential equations (ODEs) arises in modeling genuine materials' electric and mechanical behavior and describing the geological formations' rheological type. As a result, fractional ODEs have become increasingly important and famous, representing practical tools for a wide range of scientific

and engineering fields. In particular, fractional ODEs can simulate various physical phenomena realistically [1, 2]. Over the past few decades, substantial academic work has focused on finding and describing closed-form solitary wave solutions for nonlinear partial differential equations of fractional type [3]. Consequently, they have been used effectively in the literature and can build exact solutions for nonlinear fractional differential equations with noticeable physical aspects. Finally, due to their frequent recurrence in various applications such as signal processing, control theory, systems identification, solid-state physics, condensed matter physics, plasma physics, optical fibers, chemical kinetics, electrical circuits, bio-genetics and fluid dynamics, among others, nonlinear fractional equations have attracted a lot of attention among researchers [4, 5]. Providing closed-form wave solutions to these equations helps us understand these phenomena and find optimal ways to use them. It has been suggested by several investigators that there are various integral methods to find the soliton solution. These approaches are directed toward integer-order and fractional-order nonlinear PDEs [6, 7]. Most nonlinear scientific problems are approached in various multi-methodological cases, providing different visions of the tried-and-true hierarchy of relations. These cases are associated with other computational, analytical, and experiential instruments, grounding a new vision of nonlinear matters. As mentioned above, these approaches support and encourage researchers' attempts to extend existing analyses for solution candidates.

Modern scientific research has shown significant interest in the search for exact solutions related to fractional differential equations [9–12]. One of these equations, symmetric regularized long wave (SRLW) [13], has greatly interested many researchers over the years.

$$(F_{tt}) + (F_{xx}) + F_{xt}(F) + F_x F_t + F_{tt}(F_{xx}) = 0. \tag{1.1}$$

Seyler and Fenstermacher in 1984 were able to generalize the use of the SRLW equation to space-charge dynamics, long water waves, and nonlinear ion-acoustic waves [14]. Peregrine further elaborated on the significance of understanding undular bores in relation to broader wave phenomena [15]. To investigate the SRLW equation, numerous matrix and algebraic methodologies have been employed over the years: the Riemann-Hilbert scheme [16], the unified scheme [17], the Hirota bilinear form [18], and the modified simple equation methodology [19]. Furthermore, the use of ansatz methods, sub-equation method [20], the Sine-Gordon expansion method [21] and tanh-Θ/2-expansion [22] has been employed in searching for solutions of SRLW equations. Developed upon this work, our study utilizes the Riccati-Bernoulli sub-ODE method, which has not been employed in this context before. In addition, the current paper broadens the model for studying the SRLW equation to encompass fractional-order dynamics. It enriches future research directions worldwide regarding the applicability of the SRLW equation to practical fluid dynamics problems. Incorporating fractional calculus better describes the inherent memory and hereditary features inherent in modeling such systems. We also show graphical solutions that signify the relationship of the fractional order parameter to soliton dynamics to show how changes in this factor alter how waves move and the shape of solitons. The graphical representation enhances the authors' understanding of the flow of solitons in space-time fractional models. It can be useful for solving more problems related to using the SRLW equation in real-life problems, like atmospheric wave processes and weather forecasting.

Despite the plethora of studies on this subject, none of the previous works have examined the output of the Riccati-Bernoulli sub-ODE method for the equations under discussion, or addressed the applicability of the complex Bäcklund transformation. In this regard, our study provides relevant

input into the academic discourse. The present research is devoted to presenting real and intricate solutions within the framework of the Riccati-Bernoulli sub-ODE approach and contributing to the analysis of soliton behaviour, which is crucial for analyzing wave processes, including wave processes in the atmosphere. In addition, we find that shifts in solitons can be made by altering the parameters that define them [23]. This change directly affects the distance for wave propagation in atmosphere dynamics, respectively [24,25]. Further works also demonstrate this influence of varying parameters on the waves behavior [26, 27]. Additionally, the present work provides a conceptual visualization of the effect of the fractional order parameter on solitons, a visual representation to support mathematically derived conclusions regarding the effect of fractional dynamics on the wave behaviour of solitons. This study's results should help elucidate soliton features and further their use in numerical simulation of weather and other wave phenomena [28]. Specifically, our approach has aimed at the attempt to narrow the gap between mathematics and problem-solving analyses pertinent to practical usage. This has been achieved by combining theories from scientific as well as engineering disciplines [29, 30]. Other researches support relevance of this interdisciplinary link [31, 32]. We contemplate the spatial-temporal fractional formulation of the SRLW equation, denoted as Eq (1.1), expressed as follows:

$$D_{tt}^{2\alpha}(F) + D_{xx}^{2\alpha}(F) + 2D_{xt}^{2\alpha}(F)^2 + D_{xxtt}^{4\alpha}(F) = 0, \qquad 0 < \alpha \leq 1. \tag{1.2}$$

Moreover, the operator defining α-derivatives of powers is accurately consistent with the conformable fractional derivative [33]. The conformable fractional derivative provides a physically sensible and straightforward model of non-local and memory-based processes that appear in many real-world problems, such as fluid dynamics and vibrations. Classical derivatives, however, are local operators and differentiate an input concerning a small neighborhood of the point in question. At the same time, fractional derivatives also depend on past states to determine the system's current behavior. Specifically, using the conformable derivative to capture these effects is convenient. It retains essential properties such as the chain and product rules, and has a more straightforward form to apply in physical models. In the case of soliton dynamics and wave motion, the conformable fractional derivative is more suited to describing the fractional dynamics of the soliton waveforms communicating non-locally and representing the development over time. It also recreates energy dissipation and long-range dependence in wave motion more efficiently than integer-order models. Therefore, its application in this work enhances the investigation of the fractional-order dynamics of solitons and alternative nonlinear waves in fluid and atmospheric environments. Thus, conformable fractional derivatives have quickly gained popularity in recent years. It has shown that it can provide exact solutions for conformable fractional nonlinear partial differential equations using various techniques.

$$D_{\Theta}^{\alpha} Z(\Theta) = \lim_{l \to 0} \frac{Z(l(\Theta)^{1-\alpha} - Z(\theta))}{l}, 0 < \alpha \leq 1. \tag{1.3}$$

This investigation capitalizes on the following properties of this derivative:

$$\begin{cases} D_{\Theta}^{\alpha} \Theta^m = m\Theta^{m-\alpha}. \\ D_{\Theta}^{\alpha} (m_1 \eta(\Theta) \pm m_2 t(\Theta)) = m_1 D_{\Theta}^{\alpha}(\eta(\Theta)) \pm m_2 D_{\Theta}^{\alpha}(t(\Theta)). \\ D_{\Theta}^{\alpha} [f \circ g] = \Theta^{1-\alpha} g(\Theta) D_{\Theta}^{\alpha} f(g(\Theta)). \end{cases} \tag{1.4}$$

This suggested methodology is well suitable for solving complicated algebraic computations as revealed by the results above. The transformation makes extracting strict information about the

fundamental processes that underlie such complex dynamic systems feasible; conversely, it makes these processes better known. However, this method does have its own drawbacks, as discussed below. For this method to be applied, their uses are somewhat difficult, especially when the equation or the system of equations to be solved is highly nonlinear or when large amounts of computational power will be needed. Moreover, whereas exact solutions offer a rich theoretical understanding of the problem, they lack the flexibility to accommodate genuine randomness in complex and rapidly changing contexts. Still, the techniques employed in the present work provide a solid basis for future developments in analyzing such nonlinear phenomena as fluid dynamics and wave processes. The remainder of this paper is organized as follows: Section 2 is devoted to describing the methodology involved with using the Riccati-Bernoulli sub-ODE method and Bäcklund transformation. In Section 3, brief descriptions of the mathematical formulation and the main equations used in this paper are provided. The results and discussion are given in Section 4 to examine the performance of the acquired solutions. Section 5 provides concluding remarks and suggests potential difficulties for future research.

2. Algorithm

In this section, we delineate the procedural framework guiding our approach to resolving nonlinear fractional partial differential equations. Our methodology necessitates a strategy tailored to navigating the intricate complexities inherent in tackling these equations. The statement of the problem calls for a suitable approach that would help address the challenges involved in the nonlinear fractional partial differential equations.

Step 1. Consider the following fractional partial differential equation (FPDE):

$$G_1\left(g, D_t^{\alpha}(g), D_{y_1}^{\alpha}(g), D_{y_2}^{\alpha}(g), gD_{y_1}^{\alpha}(g), \ldots\right) = 0, \qquad 0 < \alpha \leq 1, \tag{2.1}$$

g is an unknown function, (G_1) is a polynomial in $(y_1, y_2, y_3, \ldots)$ and t, and all partial derivatives include nonlinear terms and higher-order derivatives. As such, complex wave paradigms and traveling wave transformation techniques are considered, which help to simplify the original expression into a form that can be used effectively.

$$G(x,t) = g(\Theta), \quad \Theta = p\frac{y_1^{\alpha}}{\alpha} + q\frac{y_2^{\alpha}}{\alpha} + r\frac{t^{\alpha}}{\alpha} \ldots + \Theta_o, \tag{2.2}$$

where $p, q, r, \ldots \Theta_o$ are constants.

Step 2. By means of a traveling wave transformation, Eq (2.1) is converted into the following nonlinear ODE:

$$G_2\left(g, g'(\Theta), g''(\Theta), gg'(\Theta), \ldots\right) = 0. \tag{2.3}$$

Step 3. With reference to the constraints $c_m \neq 0$ and $c_{-m} \neq 0$ at the same time, the presumptive solution for $g(\Theta)$ is considered, and with the Bäcklund transformation method, the solution for $\phi(\Theta)$ is obtained.

$$g(\Theta) = \sum_{i=-m}^{m} c_i \phi(\Theta)^i. \tag{2.4}$$

$$\phi(\Theta) = \frac{-\mu b + a\varphi(\Theta)}{a + b\varphi(\Theta)}. \tag{2.5}$$

With constants (μ), (a), and (b), suppose that $b \neq 0$ and introduce the function $\varphi(\Theta)$ given as:

$$\frac{d\varphi}{d\Theta} = \mu + \varphi(\Theta)^2, \tag{2.6}$$

Reference [34], shows the post-solution of Eq (2.6) and lists the conditions under which different scenarios are observed. The value of (μ) is then used to deduce the following analyses and the solution $\varphi(\Theta)$ to be derived.

$$(i) \quad \text{If} \quad \mu < 0, \quad \text{then} \quad \varphi(\Theta) = -\sqrt{-\mu}\tanh(\sqrt{-\mu}\Theta), \quad \text{or} \quad \varphi(\Theta) = -\sqrt{-\mu}\coth(\sqrt{-\mu}\Theta). \tag{2.7}$$

$$(ii) \quad \text{If} \quad \mu > 0, \quad \text{then} \quad \varphi(\Theta) = \sqrt{\mu}\tan(\sqrt{\mu}\Theta), \quad \text{or} \quad \varphi(\Theta) = -\sqrt{\mu}\cot(\sqrt{\mu}\Theta). \tag{2.8}$$

$$(iii) \quad \text{If} \quad \mu = 0, \quad \text{then} \quad \varphi(\Theta) = \frac{-1}{\Theta}. \tag{2.9}$$

Step 4. The equilibrium state following a homogeneous balance and linear polymer analysis as well as rationalization with nonlinear and higher-order derivative components are determined [35].

$$D\left[\frac{d^z g}{d\Theta^z}\right] = n + z, \quad D\left[g^j \frac{d^z g}{d\Theta^z}\right]^u = nj + u(z + n). \tag{2.10}$$

Step 5. The polynomial found from (2.5) is solved using computational tools such as Maple. Finally, substitute the values of the coefficients back to Eq (2.4) to find $g(\Theta)$.

3. Execution of the problem

We solved the space-time fractional SRLW according to the proposed approach in this section with the following waves transformation. Moreover, we conducted an examination of the formal solution pertaining to the specified FPDE. Within this context, the complex field envelope, denoted as $F(x, t)$, represents a function reliant on retarded time along the axis of prorogation.

$$\begin{aligned} \psi &= k\frac{x^\alpha}{\alpha} - \omega\frac{t^\alpha}{\alpha}. \\ F(x,t) &= f(\psi). \end{aligned} \tag{3.1}$$

Now, by employing the above complex wave transformation, Eq (1.2) is transformed into the following non-linear ODE:

$$\left(k^2 + \omega^2\right)F'' - 2\omega k\left(F^2\right)'' + \omega^2 k^2 (F)'''' = 0. \tag{3.2}$$

Upon integrating Eq (3.2) twice with respect to (ψ) and assuming the constants are zero, we obtain

$$\left(k^2 + \omega^2\right)F - 2\omega k\left(F^2\right) + \omega^2 k^2 (F)'' = 0. \tag{3.3}$$

Equation (2.10) can be utilized to determine the balance equilibrium state ($N = 2$), where the derivative term F'' is balanced with the highest-order nonlinear term F^2. Following that, substituting Eq (2.6) with Eq (2.4) into Eq (3.3) and setting the coefficients of $\phi^i(\psi)$ to zero, we have an algebraic equation system. Using Maple, we can solve this system of algebraic equations and obtain the following results:

Case 1.

$$\begin{aligned} c_0 &= 1/12\left(3\,k^2c_2+3\,\omega^2c_2+2\,\omega\,k\sqrt{-\frac{-18\,{c_2}^2k^2\omega^2-9\,{c_2}^2\omega^4-9\,{c_2}^2k^4}{4\,\omega^2k^2-16\,\omega\,kc_2}}\right)\omega^{-1}k^{-1}{c_2}^{-1},\\ c_1 &= -\sqrt[4]{-\frac{-18\,{c_2}^2k^2\omega^2-9\,{c_2}^2\omega^4-9\,{c_2}^2k^4}{4\,\omega^2k^2-16\,\omega\,kc_2}}, c_{-1}=0, c_2=c_2, c_{-2}=0, \omega=\omega, k=k,\\ \mu &= 1/3\,\sqrt{-\frac{-18\,{c_2}^2k^2\omega^2-9\,{c_2}^2\omega^4-9\,{c_2}^2k^4}{4\,\omega^2k^2-16\,\omega\,kc_2}}\omega^{-1}k^{-1}{c_2}^{-1}. \end{aligned} \tag{3.4}$$

Case 2.

$$\begin{aligned} c_0 &= \frac{2/3\,i{c_1}^2}{\omega^2}, c_1=c_1, c_{-1}=0, c_2=-1/4\,i\omega^2,\\ c_{-2} &= 0, \mu=-4/3\,\frac{{c_1}^2}{\omega^4}, b=b, \omega=\omega, k=-i\omega. \end{aligned} \tag{3.5}$$

Case 3.

$$\begin{aligned} c_0 &= c_0, c_1=0, c_{-1}=0, c_2=-32\,\frac{c_0\left(k^2-2\,\omega\,kc_0+\omega^2\right)\omega^2k^2}{\left(k^2+\omega^2-4\,\omega\,kc_0\right)^2},\\ c_{-2} &= 0, \omega=\omega, k=k, \mu=-1/8\,\frac{k^2+\omega^2-4\,\omega\,kc_0}{\omega^2k^2}. \end{aligned} \tag{3.6}$$

Case 4.

$$\begin{aligned} c_0 &= c_0, c_1=0, c_{-1}=0, c_2=1/5\,\frac{\omega\,k\left(8\,k^3\omega\,c_0+3\,\omega^4+3\,k^4+6\,\omega^2k^2+8\,\omega^3kc_0-16\,\omega^2k^2{c_0}^2\right)}{\left(k^2+\omega^2-4\,\omega\,kc_0\right)^2},\\ c_{-2} &= \frac{3}{64}\,\frac{\left(k^2+\omega^2-4\,\omega\,kc_0\right)^2}{\omega^3k^3}, \omega=\omega, k=k, \mu=-1/8\,\frac{k^2+\omega^2-4\,\omega\,kc_0}{\omega^2k^2}. \end{aligned} \tag{3.7}$$

Solution Set. 1: Thus, case 1 based on Eq (1.2) has been analyzed. Further, the following specific parameters have been used. As a result, the ensuing singular solitary wave solutions could be received under the condition ($\mu < 0$), and

$$c_0 = 1/12\left(3\,k^2c_2+3\,\omega^2c_2+2\,\omega\,k\sqrt{-\frac{-18\,{c_2}^2k^2\omega^2-9\,{c_2}^2\omega^4-9\,{c_2}^2k^4}{4\,\omega^2k^2-16\,\omega\,kc_2}}\right)\omega^{-1}k^{-1}{c_2}^{-1},$$

$$\mu = 1/3\,\sqrt{-\frac{-18\,{c_2}^2k^2\omega^2-9\,{c_2}^2\omega^4-9\,{c_2}^2k^4}{4\,\omega^2k^2-16\,\omega\,kc_2}}\omega^{-1}k^{-1}{c_2}^{-1},$$

$$F_1(x,t) = c_0 + \sqrt[4]{-\frac{-9\,c_2{}^2\omega^4 - 9\,c_2{}^2k^4 - 18\,c_2{}^2k^2\omega^2}{4\,\omega^2k^2 - 16\,\omega\,kc_2}}$$
$$\times\left(-\mu\,b - a\sqrt{-\mu}\tanh\left(\sqrt{-\mu}\left(\frac{kx^\alpha}{\alpha} - \frac{\omega\,t^\alpha}{\alpha}\right)\right)\right)\left(a - b\sqrt{-\mu}\tanh\left(\sqrt{-\mu}\left(\frac{kx^\alpha}{\alpha} - \frac{\omega\,t^\alpha}{\alpha}\right)\right)\right)^{-1}$$
$$+ c_2\left(-\mu\,b - a\sqrt{-\mu}\tanh\left(\sqrt{-\mu}\left(\frac{kx^\alpha}{\alpha} - \frac{\omega\,t^\alpha}{\alpha}\right)\right)\right)^2\left(a - b\sqrt{-\mu}\tanh\left(\sqrt{-\mu}\left(\frac{kx^\alpha}{\alpha} - \frac{\omega\,t^\alpha}{\alpha}\right)\right)\right)^{-2}, \tag{3.8}$$

or

$$F_2(x,t) = c_0 + \sqrt[4]{-\frac{-9\,c_2{}^2\omega^4 - 9\,c_2{}^2k^4 - 18\,c_2{}^2k^2\omega^2}{4\,\omega^2k^2 - 16\,\omega\,kc_2}}$$
$$\times\left(-\mu\,b - a\sqrt{-\mu}\coth\left(\sqrt{-\mu}\left(\frac{kx^\alpha}{\alpha} - \frac{\omega\,t^\alpha}{\alpha}\right)\right)\right)\left(a - b\sqrt{-\mu}\coth\left(\sqrt{-\mu}\left(\frac{kx^\alpha}{\alpha} - \frac{\omega\,t^\alpha}{\alpha}\right)\right)\right)^{-1}$$
$$+ c_2\left(-\mu\,b - a\sqrt{-\mu}\coth\left(\sqrt{-\mu}\left(\frac{kx^\alpha}{\alpha} - \frac{\omega\,t^\alpha}{\alpha}\right)\right)\right)^2\left(a - b\sqrt{-\mu}\coth\left(\sqrt{-\mu}\left(\frac{kx^\alpha}{\alpha} - \frac{\omega\,t^\alpha}{\alpha}\right)\right)\right)^{-2}. \tag{3.9}$$

Solution Set. 2: Thus, case 1 based on Eq (1.2) has been analyzed. As a result, the ensuing singular solitary wave solutions could be received under the condition ($\mu > 0$).

$$F_3(x,t) = c_0 + \sqrt[4]{-\frac{-9\,c_2{}^2\omega^4 - 9\,c_2{}^2k^4 - 18\,c_2{}^2k^2\omega^2}{4\,\omega^2k^2 - 16\,\omega\,kc_2}}$$
$$\times\left(-\mu\,b + a\sqrt{\mu}\tan\left(\sqrt{\mu}\left(\frac{kx^\alpha}{\alpha} - \frac{\omega\,t^\alpha}{\alpha}\right)\right)\right)\left(a + b\sqrt{\mu}\tan\left(\sqrt{\mu}\left(\frac{kx^\alpha}{\alpha} - \frac{\omega\,t^\alpha}{\alpha}\right)\right)\right)^{-1} \tag{3.10}$$
$$+ c_2\left(-\mu\,b + a\sqrt{\mu}\tan\left(\sqrt{\mu}\left(\frac{kx^\alpha}{\alpha} - \frac{\omega\,t^\alpha}{\alpha}\right)\right)\right)^2\left(a + b\sqrt{\mu}\tan\left(\sqrt{\mu}\left(\frac{kx^\alpha}{\alpha} - \frac{\omega\,t^\alpha}{\alpha}\right)\right)\right)^{-2},$$

or

$$F_4(x,t) = c_0 + \sqrt[4]{-\frac{-9\,c_2{}^2\omega^4 - 9\,c_2{}^2k^4 - 18\,c_2{}^2k^2\omega^2}{4\,\omega^2k^2 - 16\,\omega\,kc_2}}$$
$$\times\left(-\mu\,b - a\sqrt{\mu}\cot\left(\sqrt{\mu}\left(\frac{kx^\alpha}{\alpha} - \frac{\omega\,t^\alpha}{\alpha}\right)\right)\right)\left(a - b\sqrt{\mu}\cot\left(\sqrt{\mu}\left(\frac{kx^\alpha}{\alpha} - \frac{\omega\,t^\alpha}{\alpha}\right)\right)\right)^{-1} \tag{3.11}$$
$$+ c_2\left(-\mu\,b - a\sqrt{\mu}\cot\left(\sqrt{\mu}\left(\frac{kx^\alpha}{\alpha} - \frac{\omega\,t^\alpha}{\alpha}\right)\right)\right)^2\left(a - b\sqrt{\mu}\cot\left(\sqrt{\mu}\left(\frac{kx^\alpha}{\alpha} - \frac{\omega\,t^\alpha}{\alpha}\right)\right)\right)^{-2}.$$

Solution Set. 3: Thus, case 1 based on Eq (1.2) has been analyzed. As a result, the ensuing singular

solitary wave solutions could be received under the condition ($\mu = 0$).

$$F_5(x,t) = c_0 + \sqrt[4]{-\frac{-9\,{c_2}^2\omega^4 - 9\,{c_2}^2k^4 - 18\,{c_2}^2k^2\omega^2}{4\,\omega^2k^2 - 16\,\omega\,kc_2}} \times\left(-\mu\,b - a\left(\frac{kx^\alpha}{\alpha} - \frac{\omega\,t^\alpha}{\alpha}\right)^{-1}\right)\left(a - b\left(\frac{kx^\alpha}{\alpha} - \frac{\omega\,t^\alpha}{\alpha}\right)^{-1}\right)^{-1} + c_2\left(-\mu\,b - a\left(\frac{kx^\alpha}{\alpha} - \frac{\omega\,t^\alpha}{\alpha}\right)^{-1}\right)^2\left(a - b\left(\frac{kx^\alpha}{\alpha} - \frac{\omega\,t^\alpha}{\alpha}\right)^{-1}\right)^{-2}. \tag{3.12}$$

Solution Set. 4: Thus, case 2 based on Eq (1.2) has been analyzed. Further, the following specific parameters have been used. As a result, the ensuing singular solitary wave solutions could be received under the condition ($\mu < 0$).

$$\mu = -4/3\,\frac{{c_1}^2}{\omega^4}, \tag{3.13}$$

$$F_6(x,t) = \frac{2/3\,i{c_1}^2}{\omega^2} + c_1\left(-\mu\,b - a\sqrt{-\mu}\tanh\left(\sqrt{-\mu}\left(\frac{kx^\alpha}{\alpha} - \frac{\omega\,t^\alpha}{\alpha}\right)\right)\right)\left(a - b\sqrt{-\mu}\tanh\left(\sqrt{-\mu}\left(\frac{kx^\alpha}{\alpha} - \frac{\omega\,t^\alpha}{\alpha}\right)\right)\right)^{-1} - 1/4\,i\omega^2\left(-\mu\,b - a\sqrt{-\mu}\tanh\left(\sqrt{-\mu}\left(\frac{kx^\alpha}{\alpha} - \frac{\omega\,t^\alpha}{\alpha}\right)\right)\right)^2\left(a - b\sqrt{-\mu}\tanh\left(\sqrt{-\mu}\left(\frac{kx^\alpha}{\alpha} - \frac{\omega\,t^\alpha}{\alpha}\right)\right)\right)^{-2}, \tag{3.14}$$

or

$$F_7(x,t) = \frac{2/3\,i{c_1}^2}{\omega^2} + c_1\left(-\mu\,b - a\sqrt{-\mu}\coth\left(\sqrt{-\mu}\left(\frac{kx^\alpha}{\alpha} - \frac{\omega\,t^\alpha}{\alpha}\right)\right)\right)\left(a - b\sqrt{-\mu}\coth\left(\sqrt{-\mu}\left(\frac{kx^\alpha}{\alpha} - \frac{\omega\,t^\alpha}{\alpha}\right)\right)\right)^{-1} - 1/4\,i\omega^2\left(-\mu\,b - a\sqrt{-\mu}\coth\left(\sqrt{-\mu}\left(\frac{kx^\alpha}{\alpha} - \frac{\omega\,t^\alpha}{\alpha}\right)\right)\right)^2\left(a - b\sqrt{-\mu}\coth\left(\sqrt{-\mu}\left(\frac{kx^\alpha}{\alpha} - \frac{\omega\,t^\alpha}{\alpha}\right)\right)\right)^{-2}. \tag{3.15}$$

Solution Set. 5: Thus, case 2 based on Eq (1.2) has been analyzed. As a result, the ensuing singular solitary wave solutions could be received under the condition ($\mu > 0$).

$$F_8(x,t) = \frac{2/3\,i{c_1}^2}{\omega^2} + c_1\left(-\mu\,b + a\sqrt{\mu}\tan\left(\sqrt{\mu}\left(\frac{kx^\alpha}{\alpha} - \frac{\omega\,t^\alpha}{\alpha}\right)\right)\right)\left(a + b\sqrt{\mu}\tan\left(\sqrt{\mu}\left(\frac{kx^\alpha}{\alpha} - \frac{\omega\,t^\alpha}{\alpha}\right)\right)\right)^{-1} - 1/4\,i\omega^2\left(-\mu\,b + a\sqrt{\mu}\tan\left(\sqrt{\mu}\left(\frac{kx^\alpha}{\alpha} - \frac{\omega\,t^\alpha}{\alpha}\right)\right)\right)^2\left(a + b\sqrt{\mu}\tan\left(\sqrt{\mu}\left(\frac{kx^\alpha}{\alpha} - \frac{\omega\,t^\alpha}{\alpha}\right)\right)\right)^{-2}, \tag{3.16}$$

or

$$F_9(x,t) = \frac{2/3\,i{c_1}^2}{\omega^2} + c_1\left(-\mu\,b - a\sqrt{\mu}\cot\left(\sqrt{\mu}\left(\frac{kx^\alpha}{\alpha} - \frac{\omega\,t^\alpha}{\alpha}\right)\right)\right)\left(a - b\sqrt{\mu}\cot\left(\sqrt{\mu}\left(\frac{kx^\alpha}{\alpha} - \frac{\omega\,t^\alpha}{\alpha}\right)\right)\right)^{-1} - 1/4\,i\omega^2\left(-\mu\,b - a\sqrt{\mu}\cot\left(\sqrt{\mu}\left(\frac{kx^\alpha}{\alpha} - \frac{\omega\,t^\alpha}{\alpha}\right)\right)\right)^2\left(a - b\sqrt{\mu}\cot\left(\sqrt{\mu}\left(\frac{kx^\alpha}{\alpha} - \frac{\omega\,t^\alpha}{\alpha}\right)\right)\right)^{-2}. \tag{3.17}$$

Solution Set. 6: Thus, case 2 based on Eq (1.2) has been analyzed. As a result, the ensuing singular solitary wave solutions could be received under the condition ($\mu = 0$).

$$\begin{aligned} F_{10}(x,t) =& \frac{2/3\, ic_1{}^2}{\omega^2} + c_1\left(-\mu\, b - a\left(\frac{kx^\alpha}{\alpha} - \frac{\omega\, t^\alpha}{\alpha}\right)^{-1}\right)\left(a - b\left(\frac{kx^\alpha}{\alpha} - \frac{\omega\, t^\alpha}{\alpha}\right)^{-1}\right)^{-1} \\ & - 1/4\, i\omega^2\left(-\mu\, b - a\left(\frac{kx^\alpha}{\alpha} - \frac{\omega\, t^\alpha}{\alpha}\right)^{-1}\right)^2\left(a - b\left(\frac{kx^\alpha}{\alpha} - \frac{\omega\, t^\alpha}{\alpha}\right)^{-1}\right)^{-2}. \end{aligned} \tag{3.18}$$

Solution Set. 7: Thus, case 2 based on Eq (1.2) has been analyzed. Further, the following specific parameters have been used. As a result, the ensuing singular solitary wave solutions could be received under the condition ($\mu < 0$).

$$\mu = -1/8\, \frac{k^2 + \omega^2 - 4\,\omega\, kc_0}{\omega^2 k^2}. \tag{3.19}$$

$$F_{11}(x,t) = c_0 - \frac{32\, c_0\left(k^2 - 2\,\omega\, kc_0 + \omega^2\right)\omega^2 k^2\left(-\mu\, b - a\sqrt{-\mu}\tanh\left(\sqrt{-\mu}\left(\frac{kx^\alpha}{\alpha} - \frac{\omega\, t^\alpha}{\alpha}\right)\right)\right)^2}{\left(k^2 + \omega^2 - 4\,\omega\, kc_0\right)^2\left(a - b\sqrt{-\mu}\tanh\left(\sqrt{-\mu}\left(\frac{kx^\alpha}{\alpha} - \frac{\omega\, t^\alpha}{\alpha}\right)\right)\right)^2}, \tag{3.20}$$

or

$$F_{12}(x,t) = c_0 - \frac{32\, c_0\left(k^2 - 2\,\omega\, kc_0 + \omega^2\right)\omega^2 k^2\left(-\mu\, b - a\sqrt{-\mu}\coth\left(\sqrt{-\mu}\left(\frac{kx^\alpha}{\alpha} - \frac{\omega\, t^\alpha}{\alpha}\right)\right)\right)^2}{\left(k^2 + \omega^2 - 4\,\omega\, kc_0\right)^2\left(a - b\sqrt{-\mu}\coth\left(\sqrt{-\mu}\left(\frac{kx^\alpha}{\alpha} - \frac{\omega\, t^\alpha}{\alpha}\right)\right)\right)^2}. \tag{3.21}$$

Solution Set. 8: Thus, case 2 based on Eq (1.2) has been analyzed. As a result, the ensuing singular solitary wave solutions could be received under the condition ($\mu > 0$).

$$F_{13}(x,t) = c_0 - \frac{32\, c_0\left(k^2 - 2\,\omega\, kc_0 + \omega^2\right)\omega^2 k^2\left(-\mu\, b + a\sqrt{\mu}\tan\left(\sqrt{\mu}\left(\frac{kx^\alpha}{\alpha} - \frac{\omega\, t^\alpha}{\alpha}\right)\right)\right)^2}{\left(k^2 + \omega^2 - 4\,\omega\, kc_0\right)^2\left(a + b\sqrt{\mu}\tan\left(\sqrt{\mu}\left(\frac{kx^\alpha}{\alpha} - \frac{\omega\, t^\alpha}{\alpha}\right)\right)\right)^2}, \tag{3.22}$$

or

$$F_{14}(x,t) = c_0 - \frac{32\, c_0\left(k^2 - 2\,\omega\, kc_0 + \omega^2\right)\omega^2 k^2\left(-\mu\, b - a\sqrt{\mu}\cot\left(\sqrt{\mu}\left(\frac{kx^\alpha}{\alpha} - \frac{\omega\, t^\alpha}{\alpha}\right)\right)\right)^2}{\left(k^2 + \omega^2 - 4\,\omega\, kc_0\right)^2\left(a - b\sqrt{\mu}\cot\left(\sqrt{\mu}\left(\frac{kx^\alpha}{\alpha} - \frac{\omega\, t^\alpha}{\alpha}\right)\right)\right)^2}. \tag{3.23}$$

Solution Set. 9: Thus, case 2 based on Eq (1.2) has been analyzed. As a result, the ensuing singular solitary wave solutions could be received under the condition ($\mu = 0$).

$$F_{15}(x,t) = c_0 - \frac{32\, c_0\left(k^2 - 2\,\omega\, kc_0 + \omega^2\right)\omega^2 k^2\left(-\mu\, b - a\left(\frac{kx^\alpha}{\alpha} - \frac{\omega\, t^\alpha}{\alpha}\right)^{-1}\right)^2}{\left(k^2 + \omega^2 - 4\,\omega\, kc_0\right)^2\left(a - b\left(\frac{kx^\alpha}{\alpha} - \frac{\omega\, t^\alpha}{\alpha}\right)^{-1}\right)^2}. \tag{3.24}$$

Solution Set. 10: Thus, case 2 based on Eq (1.2) has been analyzed. Further, the following specific parameters have been used. As a result, the ensuing singular solitary wave solutions could be received under the condition ($\mu < 0$), and

$$c_2 = 1/5\,\frac{\omega\,k\left(8\,k^3\omega\,c_0 + 3\,\omega^4 + 3\,k^4 + 6\,\omega^2k^2 + 8\,\omega^3kc_0 - 16\,\omega^2k^2{c_0}^2\right)}{\left(k^2+\omega^2-4\,\omega\,kc_0\right)^2},$$

$$\mu = -1/8\,\frac{k^2+\omega^2-4\,\omega\,kc_0}{\omega^2k^2},$$

$$\begin{aligned} F_{16}(x,t) = {} & \frac{\frac{3}{64}\left(k^2+\omega^2-4\,\omega\,kc_0\right)^2\left(a-b\sqrt{-\mu}\tanh\left(\sqrt{-\mu}\left(\frac{kx^\alpha}{\alpha}-\frac{\omega\,t^\alpha}{\alpha}\right)\right)\right)^2}{\omega^3k^3\left(-\mu\,b-a\sqrt{-\mu}\tanh\left(\sqrt{-\mu}\left(\frac{kx^\alpha}{\alpha}-\frac{\omega\,t^\alpha}{\alpha}\right)\right)\right)^2} \\ & + c_0 + \frac{c_2\left(-\mu\,b-a\sqrt{-\mu}\tanh\left(\sqrt{-\mu}\left(\frac{kx^\alpha}{\alpha}-\frac{\omega\,t^\alpha}{\alpha}\right)\right)\right)^2}{\left(a-b\sqrt{-\mu}\tanh\left(\sqrt{-\mu}\left(\frac{kx^\alpha}{\alpha}-\frac{\omega\,t^\alpha}{\alpha}\right)\right)\right)^2}, \end{aligned} \tag{3.25}$$

or

$$\begin{aligned} F_{17}(x,t) = {} & \frac{\frac{3}{64}\left(k^2+\omega^2-4\,\omega\,kc_0\right)^2\left(a-b\sqrt{-\mu}\coth\left(\sqrt{-\mu}\left(\frac{kx^\alpha}{\alpha}-\frac{\omega\,t^\alpha}{\alpha}\right)\right)\right)^2}{\omega^3k^3\left(-\mu\,b-a\sqrt{-\mu}\coth\left(\sqrt{-\mu}\left(\frac{kx^\alpha}{\alpha}-\frac{\omega\,t^\alpha}{\alpha}\right)\right)\right)^2} \\ & + c_0 + \frac{c_2\left(-\mu\,b-a\sqrt{-\mu}\coth\left(\sqrt{-\mu}\left(\frac{kx^\alpha}{\alpha}-\frac{\omega\,t^\alpha}{\alpha}\right)\right)\right)^2}{\left(a-b\sqrt{-\mu}\coth\left(\sqrt{-\mu}\left(\frac{kx^\alpha}{\alpha}-\frac{\omega\,t^\alpha}{\alpha}\right)\right)\right)^2}. \end{aligned} \tag{3.26}$$

Solution Set. 11: Thus, case 2 based on Eq (1.2) has been analyzed. As a result, the ensuing singular solitary wave solutions could be received under the condition ($\mu > 0$).

$$\begin{aligned} F_{18}(x,t) = {} & \frac{\frac{3}{64}\left(k^2+\omega^2-4\,\omega\,kc_0\right)^2\left(a+b\sqrt{\mu}\tan\left(\sqrt{\mu}\left(\frac{kx^\alpha}{\alpha}-\frac{\omega\,t^\alpha}{\alpha}\right)\right)\right)^2}{\omega^3k^3\left(-\mu\,b+a\sqrt{\mu}\tan\left(\sqrt{\mu}\left(\frac{kx^\alpha}{\alpha}-\frac{\omega\,t^\alpha}{\alpha}\right)\right)\right)^2} \\ & + c_0 + \frac{c_2\left(-\mu\,b+a\sqrt{\mu}\tan\left(\sqrt{\mu}\left(\frac{kx^\alpha}{\alpha}-\frac{\omega\,t^\alpha}{\alpha}\right)\right)\right)^2}{\left(a+b\sqrt{\mu}\tan\left(\sqrt{\mu}\left(\frac{kx^\alpha}{\alpha}-\frac{\omega\,t^\alpha}{\alpha}\right)\right)\right)^2}, \end{aligned} \tag{3.27}$$

or

$$\begin{aligned} F_{19}(x,t) = {} & \frac{\frac{3}{64}\left(k^2+\omega^2-4\,\omega\,kc_0\right)^2\left(a-b\sqrt{\mu}\cot\left(\sqrt{\mu}\left(\frac{kx^\alpha}{\alpha}-\frac{\omega\,t^\alpha}{\alpha}\right)\right)\right)^2}{\omega^3k^3\left(-\mu\,b-a\sqrt{\mu}\cot\left(\sqrt{\mu}\left(\frac{kx^\alpha}{\alpha}-\frac{\omega\,t^\alpha}{\alpha}\right)\right)\right)^2} \\ & + c_0 + \frac{c_2\left(-\mu\,b-a\sqrt{\mu}\cot\left(\sqrt{\mu}\left(\frac{kx^\alpha}{\alpha}-\frac{\omega\,t^\alpha}{\alpha}\right)\right)\right)^2}{\left(a-b\sqrt{\mu}\cot\left(\sqrt{\mu}\left(\frac{kx^\alpha}{\alpha}-\frac{\omega\,t^\alpha}{\alpha}\right)\right)\right)^2}. \end{aligned} \tag{3.28}$$

Solution Set. 12: Thus, case 2 based on Eq (1.2) has been analyzed. As a result, the ensuing singular solitary wave solutions could be received under the condition ($\mu = 0$).

$$F_{20}(x,t) = \frac{\frac{3}{64}\left(k^2+\omega^2-4\,\omega\,kc_0\right)^2\left(a-b\left(\frac{kx^\alpha}{\alpha}-\frac{\omega\,t^\alpha}{\alpha}\right)^{-1}\right)^2}{\omega^3k^3\left(-\mu\,b-a\left(\frac{kx^\alpha}{\alpha}-\frac{\omega\,t^\alpha}{\alpha}\right)^{-1}\right)^2} + c_0 + \frac{c_2\left(-\mu\,b-a\left(\frac{kx^\alpha}{\alpha}-\frac{\omega\,t^\alpha}{\alpha}\right)^{-1}\right)^2}{\left(a-b\left(\frac{kx^\alpha}{\alpha}-\frac{\omega\,t^\alpha}{\alpha}\right)^{-1}\right)^2}. \tag{3.29}$$

4. Results and discussion

This investigation seeks to develop a new scientific method deeply rooted in a powerful framework to decompose the fractional SRLW equation. The equation, expressed in terms of fractional derivatives, is a daunting task with sophisticated techniques to be employed due to its complexity. Using Bäcklund transformation, fractional partial differential equations are transformed into ODEs that are transformation-friendly through additional methods. This enables a thorough examination of equation solutions. Additionally, the resolution of the equation system and its series solutions are provided. The solutions are decomposed via the Riccati-Bernoulli sub-ODE algorithm. Three families of solutions are obtained: hyperbolic, rational, and trigonometric. Consequently, a variety of analytical solutions, all different, are obtained that are a reflection of the several mathematical structures present in the fractional SRLW equation. In Tables 1 and 2, we emphasize on the distinctions between our technique and the traditional Sine-Gordon and modified extended tanh methods on the same model. Our method provides a wider spectrum of solutions, including trigonometric, hyperbolic, and rational, whereas the Sine-Gordon type equation only produces hyperbolic and modified tanh functions. This shows how our approach is more general than the standard approach, and thus capable of capturing a greater variety of physical situations. Furthermore, while the Sine-Gordon method studies the model in the time-fractional setup, our work broadens the examination of the model to the space-time fractional context, offering a more encompassing discussion of the model behavior.

The several solutions obtained in this work, including integer and fractional order solutions, present different kinds of solitary wave phenomena, as kink, anti-kink, periodic, and breather-like profiles, which have physical significances. In optical fiber communications, periodic solitons are critical because they prevent information from being distorted during transmission over long distances, and kink solitons are critical for understanding topological line solitons in particle physics and dislocations in solids. Anti-kink solitons are appropriate for developing the stone-like phenomena for further examination in condensed particle physics, particularly for cracks in nanostructures or biological tissue. The fractional-order analysis expands the research at hand by providing more precise descriptions of waves in complex physical structures where multi-scaling and time-memory interactions are important. We believe that this new approach, which differs from the earlier methods confined to integer-order models, offers fresh perspectives on soliton behavior and their possible use; this explains the novelty of our work. The comparison table and graphical solutions provided in the present study clearly reveal the specificity of these findings as compared to previous studies. Additionally, breather solitons have been crucial for nonlinear optics and oceanography, where they appear as rogue waves and produce short light pulses when they encounter a beam. Using the software environment MATLAB, we have applied meticulous adjustments of specific parameter values to accurately match the exact solutions, allowing the different periodic and single solutions to be described. As a result, the following graphical depictions provide sufficient material to make them real and comprehend the properties of solutions, hence being more capable of analyzing their dynamism.

Table 1. Comparison of the fractional SRLW with the alternative approach, specifically the modified extended tanh method.

	present method	modified extended tanh method [13]
Case I: $\eta < 0$	$F_{12}(x,t) = c_0 - \frac{32\,c_0\left(k^2-2\,\omega\,kc_0+\omega^2\right)\omega^2k^2\left(-\mu\,b-a\,\sqrt{-\mu}\coth\left(\sqrt{-\mu}\left(\frac{kx^\alpha}{\alpha}-\frac{\omega t^\alpha}{\alpha}\right)\right)\right)^2}{\left(k^2+\omega^2-4\,\omega\,kc_0\right)^2\left(a-b\,\sqrt{-\mu}\coth\left(\sqrt{-\mu}\left(\frac{kx^\alpha}{\alpha}-\frac{\omega t^\alpha}{\alpha}\right)\right)\right)^2}$	$u(x,t) = \pm\frac{i(kp-r)}{k^{3/2}\sqrt{-2qrb}}\coth\left(\sqrt{-b}\left(k\frac{x^\alpha}{\alpha}-r\frac{t^\alpha}{\alpha}\right)\right)$ for $b<0$
Case II: $\eta > 0$	$F_{14}(x,t) = c_0 - \frac{32\,c_0\left(k^2-2\,\omega\,kc_0+\omega^2\right)\omega^2k^2\left(-\mu\,b-a\,\sqrt{\mu}\cot\left(\sqrt{\mu}\left(\frac{kx^\alpha}{\alpha}-\frac{\omega t^\alpha}{\alpha}\right)\right)\right)^2}{\left(k^2+\omega^2-4\,\omega\,kc_0\right)^2\left(a-b\,\sqrt{\mu}\cot\left(\sqrt{\mu}\left(\frac{kx^\alpha}{\alpha}-\frac{\omega t^\alpha}{\alpha}\right)\right)\right)^2}$	$u(x,t) = \pm\frac{i(kp-r)}{k^{3/2}\sqrt{2qrb}}\cot\left(\sqrt{b}\left(k\frac{x^\alpha}{\alpha}-r\frac{t^\alpha}{\alpha}\right)\right)$ for $b>0$
Case III: $\eta = 0$	$F_5(x,t) = c_0 + \frac{\sqrt[4]{-\frac{-9\,c_2{}^2\omega^4-9\,c_2{}^2k^4-18\,c_2{}^2k^2\omega^2}{4\,\omega^2k^2-16\,\omega\,kc_2}}\left(-\mu\,b-a\left(\frac{kx^\alpha}{\alpha}-\frac{\omega t^\alpha}{\alpha}\right)^{-1}\right)}{\left(a-b\left(\frac{kx^\alpha}{\alpha}-\frac{\omega t^\alpha}{\alpha}\right)^{-1}\right)^{-1}} + \frac{c_2\left(-\mu\,b-a\left(\frac{kx^\alpha}{\alpha}-\frac{\omega t^\alpha}{\alpha}\right)^{-1}\right)^2}{\left(a-b\left(\frac{kx^\alpha}{\alpha}-\frac{\omega t^\alpha}{\alpha}\right)^{-1}\right)^2}$	For $b=0$, no solutions were obtained using the modified extended tanh approach for the fractional SRLW equation

Table 2. Comparison of the fractional SRLW with the alternative approach, specifically the Sine-Gordon expansion method.

	present method	Sine-Gordon expansion method [21]
Case I: $\eta < 0$	$F_{11}(x,t) = c_0\frac{-32\,c_0\left(k^2-2\,\omega\,kc_0+\omega^2\right)\omega^2k^2\left(-\mu\,b-a\,\sqrt{-\mu}\tanh\left(\sqrt{-\mu}\left(\frac{kx^\alpha}{\alpha}-\frac{\omega t^\alpha}{\alpha}\right)\right)\right)^2}{\left(k^2+\omega^2-4\,\omega\,kc_0\right)^2\left(a-b\,\sqrt{-\mu}\tanh\left(\sqrt{-\mu}\left(\frac{kx^\alpha}{\alpha}-\frac{\omega t^\alpha}{\alpha}\right)\right)\right)^2}$	$u_1(x,t) = -\frac{6a^2rv}{q} + \frac{6a^2rv}{q}i\tanh\left(a\left(x-v\frac{t^\alpha}{\alpha}\right)\right)\operatorname{sech}\left(a\left(x-v\frac{t^\alpha}{\alpha}\right)\right) + \frac{6a^2rv}{q}\tanh^2\left(a\left(x-v\frac{t^\alpha}{\alpha}\right)\right)$ for $v=\frac{p}{ra^2+1}$
Case II: $\eta > 0$	$F_{13}(x,t) = c_0 - \frac{32\,c_0\left(k^2-2\,\omega\,kc_0+\omega^2\right)\omega^2k^2\left(-\mu\,b+a\,\sqrt{\mu}\tan\left(\sqrt{\mu}\left(\frac{kx^\alpha}{\alpha}-\frac{\omega t^\alpha}{\alpha}\right)\right)\right)^2}{\left(k^2+\omega^2-4\,\omega\,kc_0\right)^2\left(a+b\,\sqrt{\mu}\tan\left(\sqrt{\mu}\left(\frac{kx^\alpha}{\alpha}-\frac{\omega t^\alpha}{\alpha}\right)\right)\right)^2}$	$u_2(x,t) = \frac{(8ra^2-1)v+p}{q} + \frac{12a^2rv}{q}\tanh^2\left(a\left(x-v\frac{t^\alpha}{\alpha}\right)\right)$
Case III: $\eta = 0$	$F_{15}(x,t) = c_0 - \frac{32\,c_0\left(k^2-2\,\omega\,kc_0+\omega^2\right)\omega^2k^2\left(-\mu\,b-a\left(\frac{kx^\alpha}{\alpha}-\frac{\omega t^\alpha}{\alpha}\right)^{-1}\right)^2}{\left(k^2+\omega^2-4\,\omega\,kc_0\right)^2\left(a-b\left(\frac{kx^\alpha}{\alpha}-\frac{\omega t^\alpha}{\alpha}\right)^{-1}\right)^2}$	$u_3(x,t) = -\frac{4a^2rv}{q} + \frac{6a^2rv}{q}i\tanh\left(a\left(x-v\frac{t^\alpha}{\alpha}\right)\right)\operatorname{sech}\left(a\left(x-v\frac{t^\alpha}{\alpha}\right)\right) + \frac{6a^2rv}{q}\tanh^2\left(a\left(x-v\frac{t^\alpha}{\alpha}\right)\right)$ for $v=\frac{-p}{4ra^2+1}$

In Figure 1, we represent a detailed visualization of solution (F_1), including its real and imaginary parts. Overall, solution (F_1) has been accurately portrayed in lump-type kink and grey kink structure plots in terms of its evolution and transformation with respect to different spatial and temporal scaling. Hence, through various spatial and temporal scaling, (F_1) demonstrates intricate behaviors that are not necessarily evident from simplistic graphs. This solution notably demonstrates propagation along the x-axis as time elapses, which retains its shape and amplitude. Notably, the way (F_1) propagates depends on the parameter (α). It could be realized that the changes in the value of the parameter (α) have an impact over the solution (F_1)'s propagation characteristics, such as wave speed and amplitude. In this relationship, one is able to appreciate the part played by fractional order with regard to the dynamics of nonlinear waves. In general, analyzing this figure contributes to gaining an understanding of real-life processes, such as fluid dynamics, soliton theory, and wave propagation.

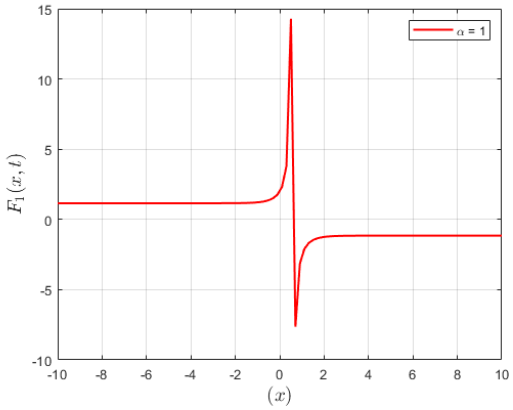

(a) $2D$ representation of the real component of (F_1) providing insight into the physical manifestations of the underlying phenomenon.

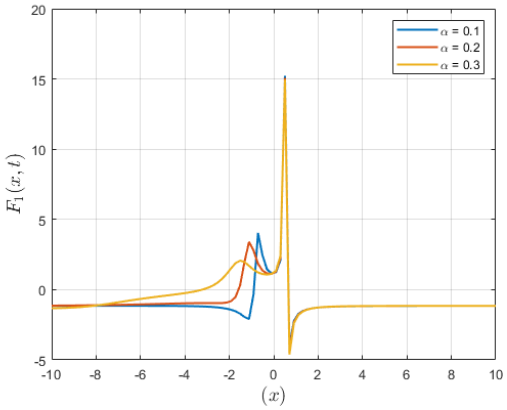

(b) Depiction of the real component of the solution (F_1), showcasing variations relative to (α), elucidating its influence on the system characteristics.

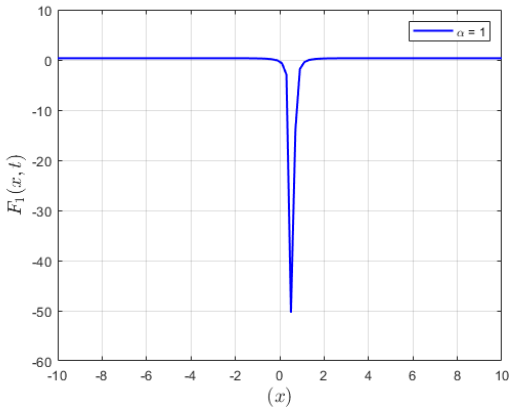

(c) $2D$ visualization of the imaginary component of the (F_1) highlighting the complex nature of the system under investigation.

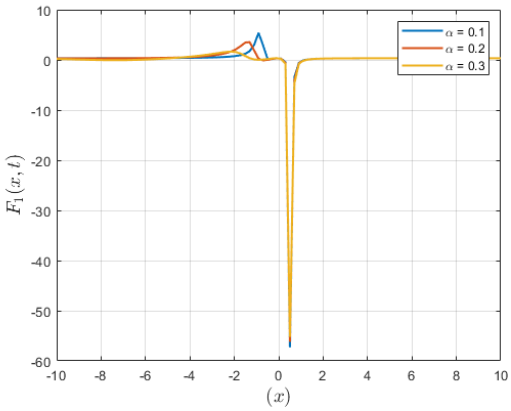

(d) $2D$ graphical representation of the imaginary component of (F_1) demonstrating its dependence on (α) and its impact on the system complex dynamics.

Figure 1. Visualization illustrating both the real and imaginary components of solution (F_1), offering a comprehensive portrayal of the system behavior and dynamics.

In Figure 2, we simulate solution (F_6) for different values of (α) using a variety of parametric configurations. (F_6) for $\alpha = 0.1, 0.2, 0.3$ shows propagation along the x-axis, remaining in the same shape and amplitude during the simulation. However, the nature of propagation is different between different values of (α). For $\alpha < 1$, as shown, the propagation is not linear. The non-linearity is observed when considering that the propagation appears to have varying speeds and does not continue at the same constant speed. On the other hand, it presented at $\alpha = 1$.

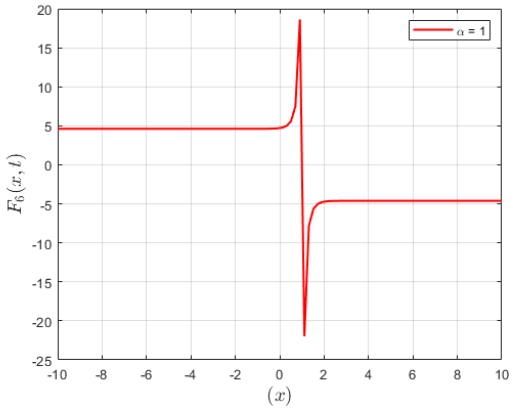

(a) $2D$ representation of the real component of (F_6) providing insight into the physical manifestations of the underlying phenomenon.

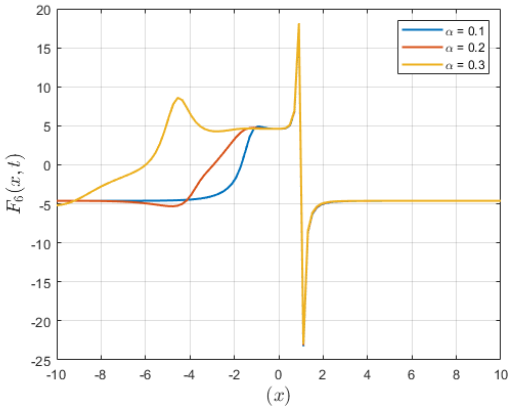

(b) Depiction of the real component of the solution (F_6), showcasing variations relative to (α), elucidating its influence on the system characteristics.

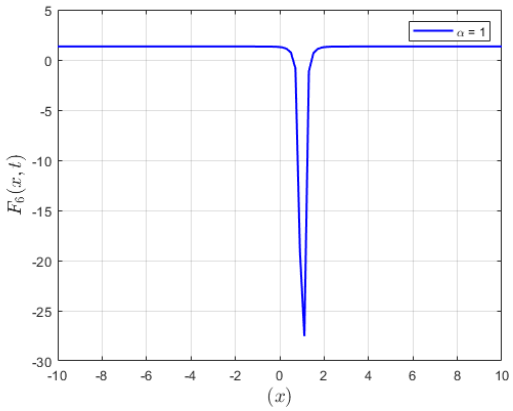

(c) $2D$ visualization of the imaginary component of the (F_6) highlighting the complex nature of the system under investigation.

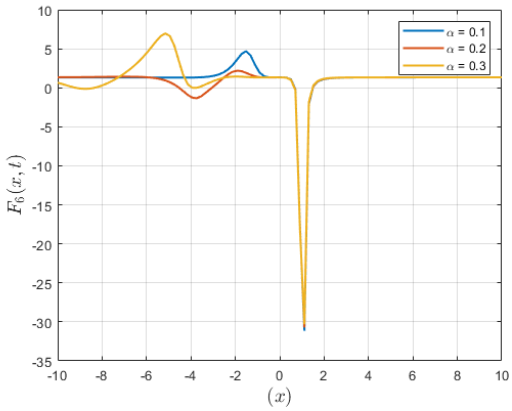

(d) $2D$ graphical representation of the imaginary component of (F_6) demonstrating its dependence on (α) and its impact on the system complex dynamics.

Figure 2. Visualization illustrating both the real and imaginary components of solution (F_6), offering a comprehensive portrayal of the system behavior and dynamics.

In Figures 3 and 4 we illustrate the relationship between the real and imaginary parts of solution (F_{10}) at different levels of granularity. By presenting kink and grey kink data, this visualization allows one to obtain a thorough understanding of the fundamental features and behavior in time of this solution at different stages and scales. Notably, the propagation of (F_{10}) is dependent on the value of (α). This

parameter determines the dynamic features of the solution and, as a result, determines the behavior of its propagation. Thus, this figure clearly shows how the dynamics of the solution (F_{10}) depend on the value of (α) in both temporal and spatial domains. In particular, propagation characteristics of (F_{10}) strongly depend on the value of (α). Variations in (α) reflect alterations in the overall nature of the solution, with respect to the rates involved and their magnitudes. This relationship clearly points to the centrality of fractional order in the description of wave nonlinear behaviors. The conclusions drawn from analysis of this figure are useful in interpreting the effects of parameters such as (α) for practical cases in fluid dynamics and wave propagation applications.

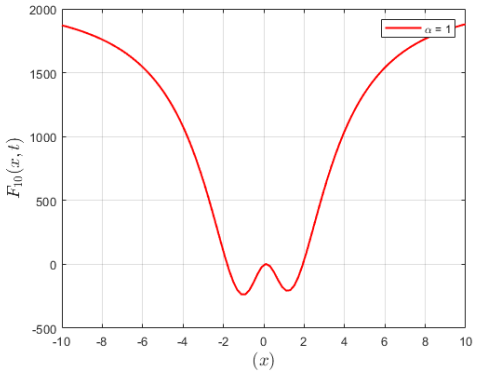

(a) $2D$ representation of the real component of (F_{10}) providing insight into the physical manifestations of the underlying phenomenon.

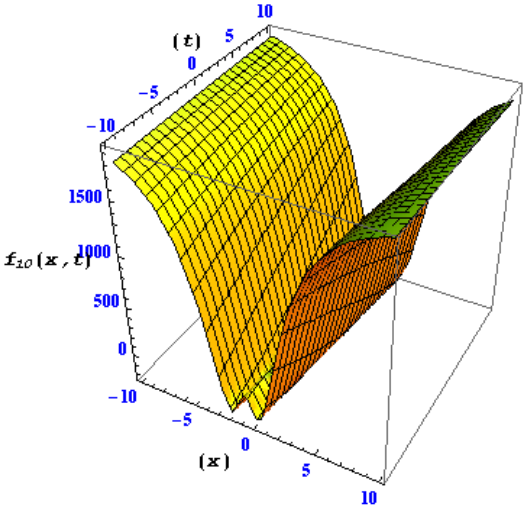

(b) $3D$ representation of the real component of (F_{10}) providing insight into the physical manifestations of the underlying phenomenon.

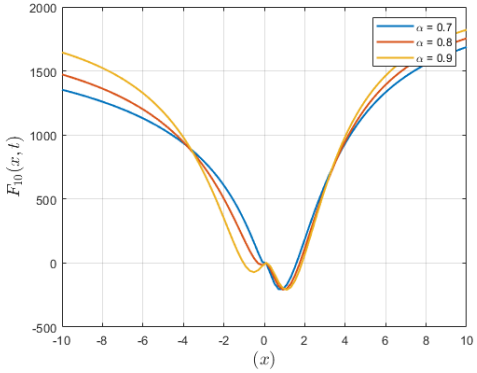

(c) $2D$ representation of the real component of (F_{10}) providing insight into the physical manifestations of the underlying phenomenon.

Figure 3. Visualization illustrating the real components of solution (F_{10}), offering a comprehensive portrayal of the system behavior and dynamics.

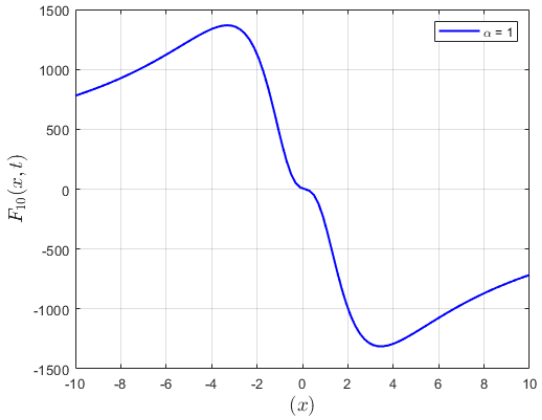

(a) $2D$ representation of the Imag component of (F_{10}) providing insight into the physical manifestations of the underlying phenomenon.

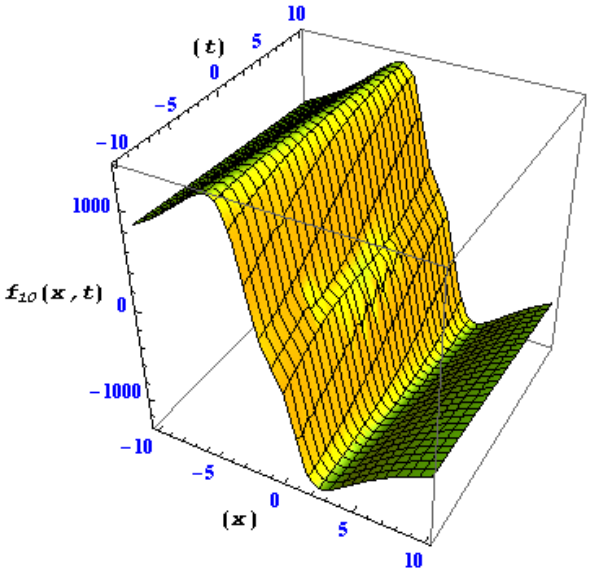

(b) $3D$ representation of the Imag component of (F_{10}) providing insight into the physical manifestations of the underlying phenomenon.

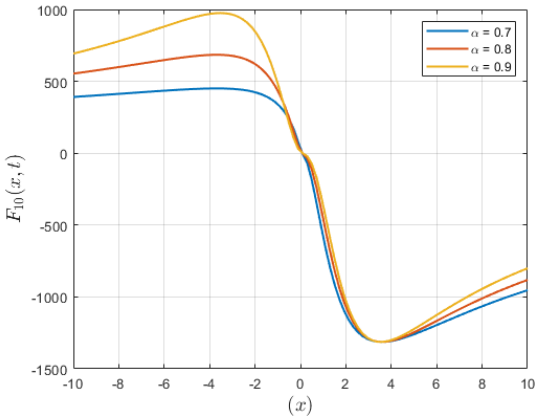

(c) $2D$ representation of the Imag component of (F_{10}) providing insight into the physical manifestations of the underlying phenomenon.

Figure 4. Visualization illustrating the image components of solution (F_{10}), offering a comprehensive portrayal of the system behavior and dynamics.

Figure 5 displays the graph of the function (F_{16}) for $\alpha = 0.7, 0.8, 0.9$ on a limited domain. From the observations, it can be inferred that the first pulse moves along the x-interval as it maintains both its shape and amplitude in time. However, the velocity of propagation solely depends on (α). Where $\alpha < 1$, the propagation accelerates initially, hence quickly traveling over a limited time. Later in time, the propagation velocity decreases, causing it to move slower. On the other hand, $\alpha = 1$ implies a uniform propagation velocity.

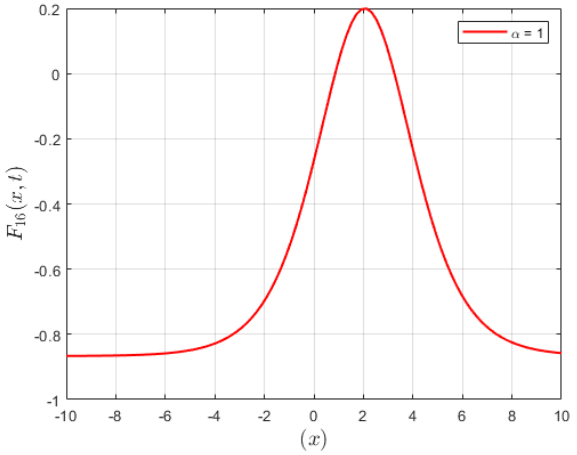

(a) $2D$ representation of the solution (F_{16}), showing its impact on the underlying physical phenomenon.

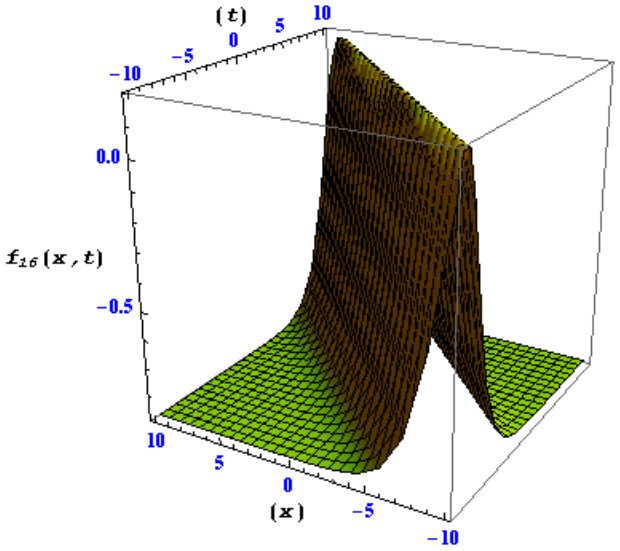

(b) $3D$ representation of the solution (F_{16}), providing insight into its complex behavior.

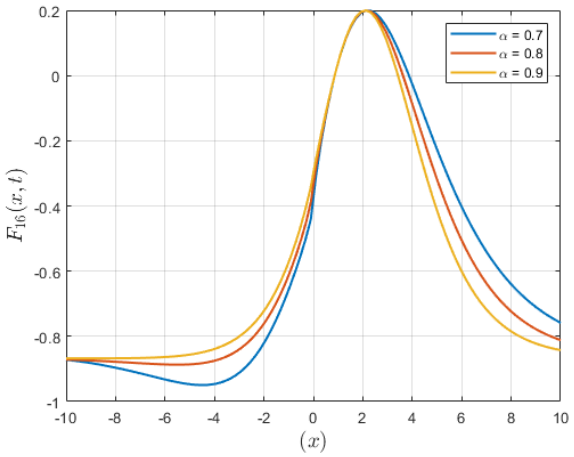

(c) Variation of the solution (F_{16}) with respect to the parameter α, highlighting its influence on system dynamics.

Figure 5. Visualizations of solution (F_{16}), offering a detailed portrayal of system behavior across different representations and parameter variations.

Figure 6 shows the evolution of solution (F_{17}), which is a bright kink soliton on various (α), varying over a finite domain of independent variables. The initial pulse is displaced along the spatial axis while retaining its form and amplitude. The only influence exerted by (α) is the speed which it moves at, due to it simply being a multipler for our time variable. For $\alpha < 1$, the pulse waves nonlinearly, however it becomes linear for $\alpha = 1$.

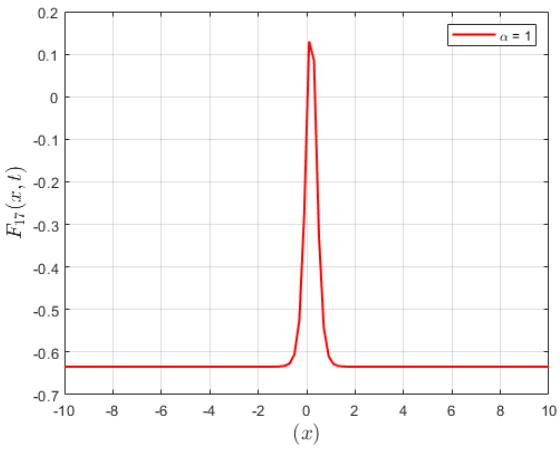

(a) $2D$ representation of (F_{17}) providing insight into the physical manifestations of the underlying phenomenon.

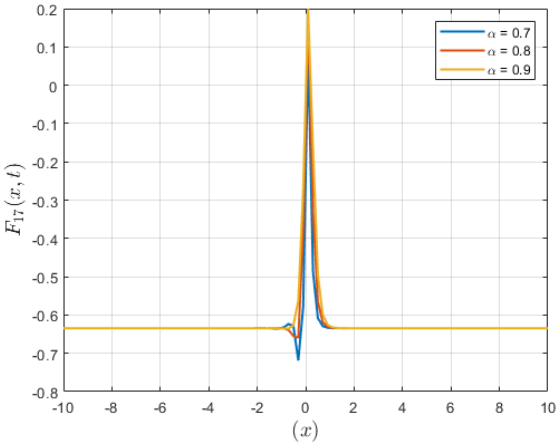

(b) Depiction of the solution (F_1), showcasing variations relative to (α), elucidating its influence on the system characteristics.

Figure 6. Visualization illustrating the solution (F_{17}), offering a comprehensive portrayal of the system behavior and dynamics.

5. Conclusions

Here, we employed the Riccati-Bernoulli sub-ODE technique, which has been identified recently as being efficient, to investigate the solitary wave solutions of the space-time fractional SRLW equation. This led us to find new exact solutions of fractional equations in trigonometric, hyperbolic, and rational forms. These findings suggest that there are research directions that can be explored to further understand these concepts. Consequently, the solutions can be used to investigate a number of physical occupations, including flow through the channels between bubbles, interactions between gravity and capillarity in thin liquid films, weakly nonlinear ion acoustic waves, and space-charges waves. Moreover, they provide information for dimensionless fluid velocity during decay situations. As far as we are aware, there is no prior work that drew similar conclusions, which speaks to the novelty of our work. This method seems to have great prospects to obtain new solitary waves in different branches of science, and to develop techniques in obstacle, free, moving, or contact problems..

In future work, it remains to apply the Riccati-Bernoulli Sub-ODE method to other types of nonlinear equations and explore the effects of other fractional orders of derivatives. Moreover, numerical simulations of the proposed solutions and the corresponding experimental verifications may give deeper understanding about their possibilities for use in fluid dynamics and waves propagations. Further efforts to analyze the applicability of the method to more complex systems or higher-dimensional models will also be considered in expanding this study.

Author contributions

Conceptualization, W.H; Data curation, A.A.A.; Formal analysis, W.H; Resources, A.A.A; Investigation, W.H; Project administration, A.A.A; Validation, W.H.; Software, A.A.A; Validation,

W.H; Visualization, A.A.A.; Validation, W.H.; Visualization, A.A.A.; Resources, W.H.; Project administration, A.A.A.; Writing–review & editing, W.H.; Funding, A.A.A. All authors have read and agreed to the published version of the manuscript.

Acknowledgments

The authors gratefully acknowledge the funding of the Deanship of Graduate Studies and Scientific Research, Jazan University, Saudi Arabia, through Project Number: GSSRD-24.

Conflict of interest

The authors declare that they have no conflicts of interest.

References

1. I. Podlubny, *Fractional differential equations: an introduction to fractional derivatives, fractional differential equations, to methods of their solution and some of their applications*, Vol. 198, Elsevier, 1999.
2. X. J. Yang, *Local fractional functional analysis and its applications*, Hong Kong: Asian Academic Publisher Limited, 2011.
3. X. J. Yang, *Advanced local fractional calculus and its applications*, World Science Publisher, 2012.
4. M. A. Khan, M. A. Akbar, N. N. binti Abd Hamid, Traveling wave solutions for space-time fractional Cahn Hilliard equation and space-time fractional symmetric regularized long-wave equation, *Alexandria Eng. J.*, **60** (2021), 1317–1324. https://doi.org/10.1016/j.aej.2020.10.053
5. M. A. Khan, M. Ali Akbar, N. H. Ali, M. U. Abbas, The new auxiliary method in the solution of the generalized Burgers-Huxley equation, *J. Prime Res. Math.*, **16** (2020), 16–26.
6. M. A. Khan, N. Alias, U. Ali, A new fourth-order grouping iterative method for the time fractional sub-diffusion equation having a weak singularity at initial time, *AIMS Math.*, **8** (2023), 13725–13746. https://doi.org/10.3934/math.2023697
7. M. A. Khan, N. Alias, I. Khan, F. M. Salama, S. M. Eldin, A new implicit high-order iterative scheme for the numerical simulation of the two-dimensional time fractional cable equation, *Sci. Rep.*, **13** (2023), 1549. https://doi.org/10.1038/s41598-023-28741-7
8. N. Cao, X. J. Yin, S. T. Bai, L. Y. Xu, Lump-soliton, rogue-soliton interaction solutions of an evolution model for magnetized Rossby waves, *Nonlinear Dyn.*, **112** (2024), 9367–9389. https://doi.org/10.1007/s11071-024-09492-0
9. P. Xu, F. T. Long, C. Shan, G. Li, F. Shi, K. J. Wang, The fractal modification of the Rosenau-Burgers equation and its fractal variational principle, *Fractals*, **32** (2024), 2450121. https://doi.org/10.1142/S0218348X24501214
10. M. A. Khatun, M. A. Arefin, M. H. Uddin, D. Baleanu, M. A. Akbar, M. Inc, Explicit wave phenomena to the couple-type fractional-order nonlinear evolution equations, *Results Phys.*, **28** (2021), 104597. https://doi.org/10.1016/j.rinp.2021.104597

11. M. H. Uddin, M. A. Akbar, M. A. Khan, M. A. Haque, Families of exact traveling wave solutions to the space-time fractional modified KdV equation and the fractional Kolmogorov-Petrovskii-Piskunov equation, *J. Mech. Cont. Math. Sci.*, **13** (2018), 17–33.

12. U. H. M. Zaman, M. A. Arefin, M. A. Akbar, M. H. Uddin, Explore dynamical soliton propagation to the fractional order nonlinear evolution equation in optical fiber systems, *Opt. Quant. Electron.*, **55** (2023), 1295. https://doi.org/10.1007/s11082-023-05474-5

13. K. K. Ali, R. I. Nuruddeen, K. R. Raslan, New structures for the space-time fractional simplified MCH and SRLW equations, *Chaos Soliton. Fract.*, **106** (2018), 304–309. https://doi.org/10.1016/j.chaos.2017.11.038

14. C. E. Seyler, D. L. Fenstermacher, A symmetric regularized long wave equation, *Phys. Fluids*, **27** (1984), 4–7. https://doi.org/10.1063/1.864487

15. D. H. Peregrine, Calculations of the development of an undular bore, *J. Fluid Mech.*, **25** (1966), 321–330. https://doi.org/10.1017/S0022112066001678

16. J. J. Yang, S. F. Tian, Z. Q. Li, Riemann-Hilbert problem for the focusing nonlinear Schrödinger equation with multiple high-order poles under nonzero boundary conditions, *Phys. D*, **432** (2022), 133162. https://doi.org/10.1016/j.physd.2022.133162

17. D. C. Nandi, M. S. Ullah, H. O. Roshid, M. Z. Ali, Application of the unified method to solve the ion sound and Langmuir waves model, *Heliyon*, **8** (2022), e10924. https://doi.org/10.1016/j.heliyon.2022.e10924

18. M. S. Ullah, O. Ahmed, M. A. Mahbub, Collision phenomena between lump and kink wave solutions to a (3 + 1)-dimensional Jimbo-Miwa-like model, *Partial Differ. Equ. Appl. Math.*, **5** (2022), 100324. https://doi.org/10.1016/j.padiff.2022.100324

19. M. S. Ullah, H. O. Roshid, M. Z. Ali, N. F. M. Noor, Novel dynamics of wave solutions for Cahn-Allen and diffusive predator-prey models using MSE scheme, *Partial Differ. Equ. Appl. Math.*, **3** (2021), 100017. https://doi.org/10.1016/j.padiff.2020.100017

20. S. F. Tian, X. F. Wang, T. T. Zang, W. H. Qiu, Stability analysis, solitary wave and explicit power series solutions of a (2 + 1)-dimensional nonlinear Schrödinger equation in a multicomponent plasma, *Int. J. Numer. Methods Heat Fluid Flow*, **3** (2021), 1732–1748. https://doi.org/10.1108/HFF-08-2020-0517

21. A. Korkmaz, O. E. Hepson, K. Hosseini, H. Rezazadeh, M. Eslami, Sine-Gordon expansion method for exact solutions to conformable time fractional equations in RLW-class, *J. King Saud Univ.-Sci.*, **32** (2020), 567–574. https://doi.org/10.1016/j.jksus.2018.08.013

22. J. Manafian, Optical soliton solutions for Schrödinger-type nonlinear evolution equations by the $\tan(\Phi(\xi)/2)$-expansion method, *Optik*, **127** (2016), 4222–4245. https://doi.org/10.1016/j.ijleo.2016.01.078

23. A. A. Alderremy, R. Shah, N. Iqbal, S. Aly, K. Nonlaopon, Fractional series solution construction for nonlinear fractional reaction-diffusion Brusselator model utilizing Laplace residual power series, *Symmetry*, **14** (2022), 1944. https://doi.org/10.3390/sym14091944

24. S. Alshammari, M. M. Al-Sawalha, R. Shah, Approximate analytical methods for a fractional-order nonlinear system of Jaulent-Miodek equation with energy-dependent Schrödinger potential, *Fractal Fract.*, **7** (2023), 140. https://doi.org/10.3390/fractalfract7020140

25. M. M. Al-Sawalha, R. Shah, A. Khan, O. Y. Ababneh, T. Botmart, Fractional view analysis of Kersten-Krasil'shchik coupled KdV-mKdV systems with non-singular kernel derivatives, *AIMS Math.*, **7** (2022), 18334–18359. https://doi.org/10.3934/math.20221010

26. H. Yasmin, A. S. Alshehry, A. H. Ganie, A. M. Mahnashi, R. Shah, Perturbed Gerdjikov-Ivanov equation: soliton solutions via Backlund transformation, *Optik*, **298** (2024), 171576. https://doi.org/10.1016/j.ijleo.2023.171576

27. M. Alqhtani, K. M. Saad, R. Shah, W. Weera, W. M. Hamanah, Analysis of the fractional-order local Poisson equation in fractal porous media, *Symmetry*, **14** (2022), 1323. https://doi.org/10.3390/sym14071323

28. M. Alqhtani, K. M. Saad, W. M. Hamanah, Discovering novel soliton solutions for (3 + 1)-modified fractional Zakharov-Kuznetsov equation in electrical engineering through an analytical approach, *Opt. Quant. Electron.*, **55** (2023), 1149. https://doi.org/10.1007/s11082-023-05407-2

29. M. Naeem, O. F. Azhar, A. M. Zidan, K. Nonlaopon, R. Shah, Numerical analysis of fractional-order parabolic equations via Elzaki transform, *J. Funct. Spaces*, **2021** (2021), 3484482. https://doi.org/10.1155/2021/3484482

30. W. Alhejaili, E. Az-Zo'bi, R. Shah, S. A. El-Tantawy, On the analytical soliton approximations to fractional forced Korteweg-de Vries equation arising in fluids and Plasmas using two novel techniques, *Commun. Theor. Phys.*, **76** (2024), 085001. https://doi.org/10.1088/1572-9494/ad53bc

31. S. Noor, W. Albalawi, R. Shah, M. M. Al-Sawalha, S. M. E. Ismaeel, S. A. El-Tantawy, On the approximations to fractional nonlinear damped Burger's-type equations that arise in fluids and plasmas using Aboodh residual power series and Aboodh transform iteration methods, *Front. Phys.*, **12** (2024), 1374481. https://doi.org/10.3389/fphy.2024.1374481

32. S. Noor, A. S. Alshehry, A. Shafee, R. Shah, Families of propagating soliton solutions for (3 + 1)-fractional Wazwaz-BenjaminBona-Mahony equation through a novel modification of modified extended direct algebraic method, *Physica Scripta*, **99** (2024), 045230. https://doi.org/10.1088/1402-4896/ad23b0

33. M. Z. Sarikaya, H. Budak, H. Usta, On generalized conformable fractional calculus, *TWMS J. Appl. Eng. Math.*, **9** (2019), 792–799.

34. D. Lu, Q. Shi, New Jacobi elliptic functions solutions for the combined KdV-mKdV equation, *Int. J. Nonlinear Sci.*, **10** (2010), 320–325.

35. Y. Zhang, Solving STO and KD equations with modified Riemann-Liouville derivative using improved (G/G')-expansion function method, *Int. J. Appl. Math.*, **45** (2015), 16–22.